ISSN 1330–0008
CODEN FIZAE4

LEAK DETECTION LIMIT OF COUNTER–FLOW TYPE LEAK DETECTOR

GEN'ICHI HORIKOSHI

National Laboratory for High Energy Physics (Emeritus Professor), Kashiwada 3322-7, Ushiku-shi, Ibaraki, 300-12, Japan

Received 7 April 1995

UDC 539.1.074

PACS 07.30.Hd

Paying attention to a two-inlet turbomolecular pump and a new counter-flow leak detector proposed by G. Reich, we made a general survey of leak-detection systems. Among many types of leak-detection systems, we selected several of them, including a system with a new type counter-flow leak detector, and analysed their performances. To evaluate leak-detection performance of the systems, minimum detectable leak and time constant of response are introduced. In terms of these quantities, we evaluate the leak-detection performance of the systems, and explore the leak-detection limit.

1. *Introduction*

Since the first proposal of counter-flow type (helium) leak detector (LD) by W. Becker [1], this type of device has widely been used in leak hunting of many vacuum components and systems. In a leak hunting system with counter-flow LD, the probe gas (helium) entering into the test chamber through a leak, travels to the sensor through high vacuum pump reversely by counter-flow process. In general, it has been wrongly considered that the counter-flow LD is less sensitive than the ordinary type LD because of the counter-flow process. G. Reich has pointed out advantages of the counter-flow LD, and proposed a new type counter-flow LD [2].

In this paper, we will analyse main mechanisms of counter-flow LD, taking into account potential advantages of counter-flow process, and propose a new version of counter-flow LD. In Fig. 1, the concept of the new version of counter–flow LD is shown. In the new version, the LD has two turbomolecular pumps (TMPs) of a small size, one is of ordinary type and the other is of a small ultimate compression ratio. Backing lines of these TMPs are connected to one forepump through a small conductance. A sensor is mounted at the inlet of the second TMP.

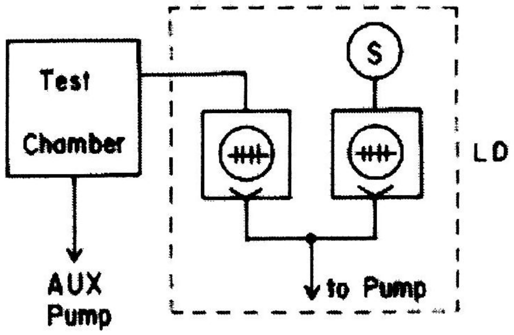

Fig. 1. A schematic diagram of the new counter-flow leak detector: S denotes the sensor and LD the leak detector.

Taking into account several types of leak–hunting systems, including a system with the new counter–flow LD, we pay attention to partial pressures of several main gas species, and estimate minimum detectable leak rate as well as response time constant for each system. It is expected that the new counter–flow LD will improve the minimum detectable leak rate by at least one or two order of magnitude compared to the ordinary LD.

We consider several typical leak testing methods and quantitatively examine merits and/or demerits of each method. Some analytical studies of these methods as well as the S/N ratio of LD output and the response time constant for each leak hunting method are analytically studied.

2. Leak detection methods

There are two types of helium LD on the market, i.e., ordinary type LD and the counter-flow type LD. Figure 2 shows a variety of leak detection methods. Figure 2a shows the simplest leak detection method that is only applicable to a small chamber. The chamber is connected directly to an ordinary LD and the vacuum pump built in the LD pumps down the chamber. Helium gas entering through a leak, if any, quickly reaches the sensor. The sensitivity is high and response time is short. In the case of Fig. 2b, the chamber to be tested is large and an auxiliary pump is necessary for pumping down the chamber. Helium gas entering the chamber flows in two directions, to the auxilliary pump and to the ID. The sensitivity of leak hunting decreases by the dividing ratio $s/(s+S)$, where s and S are the effective pumping speeds of the LD and the auxiliary pump, respectively. In some cases S is very high and this decreases the leak detection sensitivity very much. A method shown in Fig. 2c improves this point. The LD is connected to the backing line of the auxiliary high vacuum pump. In this case, the dividing ratio of $s/(s+S_B)$ is larger than that of the previous method, because S_B, the pumping speed of the forepump of the high vacuum pump, is much smaller than S. The only problem is that backing pressure of the auxiliary pump is not low enough and a regulation of gas flow to the LD is necessary to keep the pressure in LD low. This results in a decrease of sensitivity of the LD. On the other hand, because of the small volume of the forepump backside manifold of the auxiliary pump, the response time is fairly short.

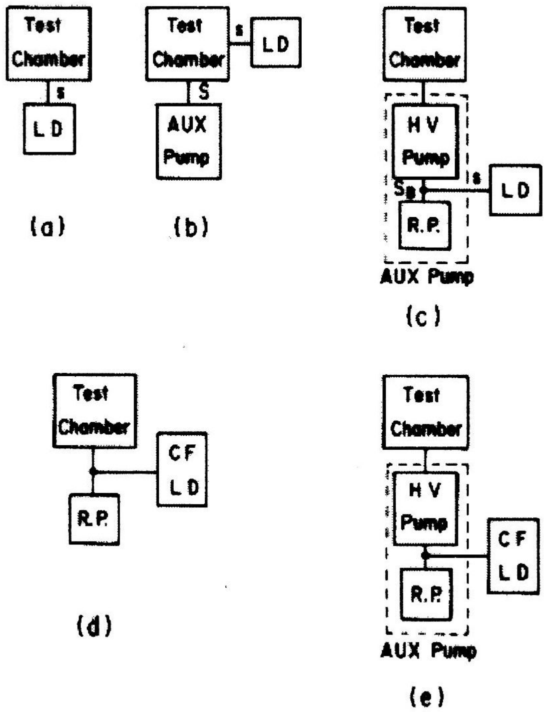

Fig. 2. Schematic diagrams of typical detector systems: ordinary leak detector (LD), rotary pump (RP), high vacuum pump (HV pump), pumping speeds (s, S, S_B), counter-flow leak detector (cf LD).

Although the counter-flow LD (Fig. 3) is less sensitive than the ordinary LD by more than one order of magnitude, it can work at much higher pressure level than an ordinary LD. Figure 2d shows a simple leak detection method with a counter-flow LD. A vacuum chamber to be tested is pumped down only by a rotary pump, and a counter flow LD is connected to the inlet part of the rotary pump. Most of helium gas entering the chamber through a leak is pumped out by the rotary pump, but a small part of it will reach the sensor of LD by counter-flowing across the turbomolecular pump (TMP) in the LD. Because the counter-flow process is the only way for helium gas to reach the sensor, it is usually said that the sensitivity of a counter-flow is about one order smaller than that of an ordinary LD. The method of Fig. 2e overcomes this difficulty. In this case, a high vacuum system composed of a high vacuum pump and a rotary pump pumps down the test chamber, and a counter flow LD is connected at the outlet of the high vacuum pump. The high vacuum pump compresses helium gas and after that a small part of it flows to the LD and finally reaches the sensor by the counter-flow process. The high-vacuum pump works as a compressor for helium gas and improves the sensitivity of the counter-flow LD.

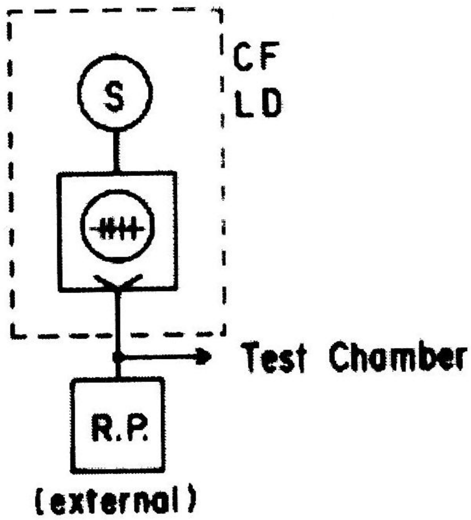

Fig. 3. A schematic diagram of the counter-flow leak detector.

Leak detection methods mentioned above, led us to the idea of a new counter-flow LD. Figure 5 shows a schematic composition of the new counter-flow LD and an example of leak detection system with a new counter-flow LD (system B). The new-counter flow LD is composed of two TMPs, one of an ordinary type (TMP-A) and the other a special type of low ultimate compression ratio (TMP-B). The outlets of these TMPs are connected to each other and to a forepump through an adjustable valve of small conductance.

Helium gas entering the chamber flows to the outlet of TMP-A and a part of it reaches the sensor at the inlet of TMP-B. The helium pressure pattern in the new counter-flow LD is as follows. The pressure in the test chamber is low, and in the first stage, the helium gas is compressed by TMP-A, then in the second stage, is diluted in the counter-flow to the sensor at the inlet of TMP-B.

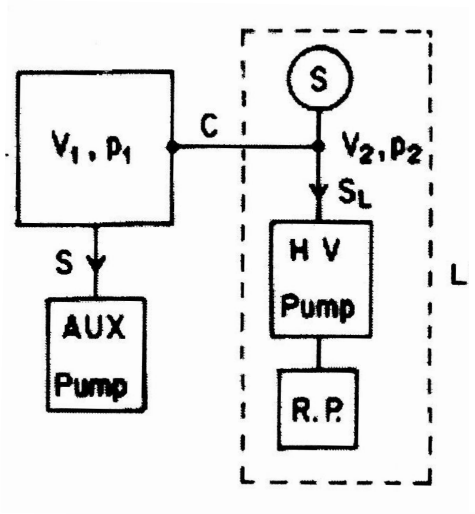

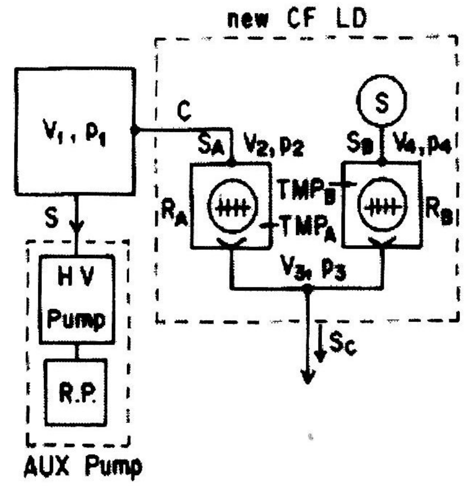

Fig. 4. A schematic diagram of the leak detection system with an ordinary leak detector (system A). Notations are listed in Table 1.

Fig. 5. A schematic diagram of the leak detection system with the new counter-flow leak detector (system B): ordinary turbomolecular pump (TMP–A), turbomolecular pump with a small ultimate compression ratio (TMP–B). Other notations are listed in Table 2 (right).

TABLE 1.
Quantities and notations used for System A (Fig. 4).

Item		Value used in example			
	Nota-tion	kind of gas species considered			
		H_2	He	water vapour	N_2
Pumping speed of aux. vac. pump	S	300 l s^{-1}			
Pumping speed of vac. pump in LD	S_L	100 l s^{-1}			
Flow cond. of connect. tube between test chamber and LD (l s^{-1})	C	7.5	5.3	2.5	2.0
Pressure in test chamber (Pa)	p_1	3.26 $\times 10^{-10}$	3.28 $\times 10^{-9}$	3.31 $\times 10^{-5}$	3.31 $\times 10^{-5}$
Pressure in sensor manifold (Pa)	p_2	3.20 $\times 10^{-11}$	1.65 $\times 10^{-10}$	1.78 $\times 10^{-6}$	3.59 $\times 10^{-6}$
Volume of test chamber	V_1	100 l			
Volume of sensor manifold	V_2	1.5 l			
Quantity of gas generation in test chamber (Pa l s^{-1})	Q_1	1×10^{-7}	1×10^{-6}	1×10^{-2}	1×10^{-2}
Quantity of gas genereration in sensor manifold (Pa l s^{-1})	Q_2	1×10^{-9}	–	1×10^{-4}	3×10^{-4}

TABLE 2.
Quantities and notations used for System B (Fig.5).

Item	Notation	Value used in example			
		kind of gas species considered			
		H_2	He	water vapour	N_2
Pump. speed of auxiliary vac. pump	S	300 l s^{-1}			
Pump. speed of TMP-A	S_A	100 l s^{-1}			
Pump. speed of TMP-B	S_B	100 l s^{-1}			
Flow conductance of connecting tube between test chamber and LD (l s^{-1})	C	7.5	5.3	2.5	2.0
Ultimate compress. ratio of TMP-A	R_A	650	5500	1×10^{8}	1×10^{10}
Ultimate compress. ratio of TMP-B	R_B	25	74	1×10^{4}	1×10^{5}
Pumping speed of forepump (l s^{-1})	S_C	0.01			
Pressure in test chamber (Pa)	p_1	3.31×10^{-10}	3.28×10^{-9}	3.31×10^{-5}	3.31×10^{-5}
Pressure at the inlet of TMP-A (Pa)	p_2	–	–	–	–
Pressure of common backing line of TMP-A (Pa)	p_3	1.64×10^{-7}	1.59×10^{-6}	1.90×10^{-2}	3.85×10^{-2}
Pressure in sensor manifold (Pa)	p_4	6.56×10^{-9}	2.15×10^{-8}	2.90×10^{-6}	3.32×10^{-6}
Volume of test chamber	V_1	100 l			
Volume of pump mouth of TMP-A	V_2	0.2 l			
Volume of common backing line and TMP-B	V_3	0.2 l			
Volume of sensor manifold	V_4	0.3 l			
Quantity of gas generation in test chamber (Pa l s^{-1})	Q_1	1×10^{-7}	1×10^{-6}	1×10^{-2}	1×10^{-2}
Quantity of gas generation in sensor manifold (Pa l s^{-1})	Q_4	1×10^{-9}	–	1×10^{-4}	3×10^{-4}

In a TMP under a constant gas flow operation, the ratio of backing pressure to the operating pressure of the pump is nearly equal to the ratio of pumping speed of the TMP to that of the forepump, but never exceeds the ultimate compression ratio. In a limiting case of no gas flow, the above pressure ratio approaches the ultimate compression ratio R. The heavier the gas molecule, the larger is R. Because the ultimate compression ratio of TMP-A is large enough for most gases, TMP-A compresses helium and other gases by the ratio of its pumping speed to that of the forepump. On the other hand, TMP-B is working without any gas flow and the compression ratio is equal to the ultimate compression ratio, i.e., the pressure at the sensor is diluted by a factor of $1/R$. Because R increases largely with mass number, partial pressure of gases other than helium at the sensor strongly decreases. Therefore, it can be said that the new counter-flow LD largely improves the signal to background noise ratio.

3. Analysis

3.1. S/N ratio

Consider two leak detection systems shown in Figs. 4 and 5. Figure 4 shows a leak detection system with an ordinary LD (system A). A chamber of volume V_1 is tested. A high vacuum pump and an ordinary LD are installed to the chamber. As mentioned above, Fig. 5 shows another system with a new type counter-flow LD (system B). A chamber of the same volume as in system A is tested. In this case, too, a vacuum pump of the same size and a new type counter-flow LD are connected to the chamber. Notations used in Figs. 4 and 5 as well as in the following analysis are summarized in Tables 1 and 2.

For the system A (Fig. 4), we have the following set of equations which relate pressure p_1 and p_2 with gas loads Q_1 and Q_2 in the system:

$$Q_1 = p_1 S + C(p_1 - p_2), \qquad (1)$$

$$Q_2 = p_2 S_L + C(p_2 - p_1),$$

where Q_1 and Q_2 are amounts of gas entering in the test chamber and the sensor manifold, respectively (or are generated in them). From Eq. (1), we obtain p_1 and p_2 as

$$p_1 = \frac{CQ_1(S_1 + C) + CQ_2}{SS_L + C(S + S_L)}, \qquad (2)$$

$$p_2 = \frac{CQ_1 + (S + C)Q_2}{SS_L + C(S + S_L)}.$$

For the system B, the network is more complex and we should treat TMPs more rigorously. We consider TMP as a directional conductance, i.e., the amount of gas flow Q through the TMP is given as

$$Q = Sp_1 - S\frac{p_2}{R}$$

where R is the ultimate compression rate, and p_1 and p_2 are pressures at the pump mouth and at exhaust flanges of TMP, respectively.

Referring to Fig. 5 and Table 2, we can give a set of relations between pressures p_1, p_2, p_3 and p_4 and gas generation (Q_1 and Q_4) by means of the matrix equation:

$$\begin{pmatrix} S + C & -C & 0 & 0 \\ -C & S_A + C & -S_A/R_A & 0 \\ 0 & -S_A & S_C + S_A/R_A + S_B & -S_B \\ 0 & 0 & -S_B/R_B & S_B \end{pmatrix} \begin{pmatrix} p_1 \\ p_2 \\ p_3 \\ p_4 \end{pmatrix} = \begin{pmatrix} Q_1 \\ Q_2 \\ Q_3 \\ Q_4 \end{pmatrix} \qquad (3)$$

where we assumed $Q_2 = Q_3 = 0$ [3]. The values of p_1, p_2, p_3 and p_4 are solutions of the matrix equation:

$$[D_{ij}]\,[Q_j] = [p_i] \quad (i = 1, 2, 3, 4), \tag{4}$$

where $[D_{ij}]$ is the inverse matrix to the one in Eq. (3). For example, p_4 is expressed as

$$p_4 = \frac{1}{\Delta}\left\{Q_1 \frac{R_A}{R_B} C S_A S_B + Q_4 \left[\left(S_C + \frac{S_B}{R_B}\right)(R_A C S_A + CS + R_A S_A S) + \frac{C S S_A}{R_A}\right]\right\},$$

where

$$\Delta = S_B R_B \left(C S S_C + C S_A S_C R_A + R_A S S_A S_C + \frac{C S_A S}{R_A}\right).$$

TABLE 3.
Signal, noise and minimum detectable leak in both cases of system A and system B.

		System A	System B ($S_C = 0.01$)	System B ($S_C = 0.03$)
Partial pressures of main gases in sensor manifold (Pa)	H_2	3.20×10^{-11}	6.56×10^{-9}	3.24×10^{-8}
	He	1.65×10^{-1}	2.15×10^{-8}	7.22×10^{-9}
	H_2O	1.78×10^{-6}	2.90×10^{-6}	1.60×10^{-6}
	N_2	3.59×10^{-6}	3.32×10^{-6}	3.10×10^{-6}
Sensor output due to each gas (reduced to helium pressure in Pa_{He})	H_2	1.60×10^{-15}	3.28×10^{-13}	1.62×10^{-12}
	He	1.65×10^{-10}	2.15×10^{-8}	7.22×10^{-9}
	H_2O	8.90×10^{-13}	1.45×10^{-12}	8.00×10^{-13}
	N_2	1.80×10^{-14}	1.66×10^{-14}	1.55×10^{-14}
Electronic fluctuation (Pa_{He})		3×10^{-13}	3×10^{-13}	3×10^{-13}
S/N ratio		136	1.0×10^{4}	2640
Minimum detectable leak L_{min} (Pa l s^{-1})		7.35×10^{-9}	1.0×10^{-10}	3.78×10^{-10}
Response time constant $\tau(s)$		0.33	8.26	3.58
$(\text{Detectability})^{-1} = \tau L_{min}$		2.43×10^{-9}	8.26×10^{-10}	1.35×10^{-9}

To have a practical view of the above analysis, we susbstitute concrete values for all components and quantities of the system as given in Tables 1 and 2. Assuming the linear velocity of rotor blade of the two TMPs is 200 m/s and the number of stage in TMP-A and TMP-B are 28 and 14, respectively, and referring to the analysis by Taniguchi et al. [4], we estimate the ultimate compression ratio of these TMPs for main gas species (see Table 3). We pay attention to four kinds of gases, i.e., hydrogen, helium, water and nitrogen (air) as gas loads. The reasons why we consider these gases in the analysis are:

(1) hydrogen is the lightest gas and most vigorous in the counter-flow process;

(2) helium is used as the probe gas;

(3) water vapour is the main desorption component, and

(4) nitrogen is the main component of leakage.

In Tables 1 and 2, typical values of Q_1 and Q_4 used in the analysis are listed for each gas species.

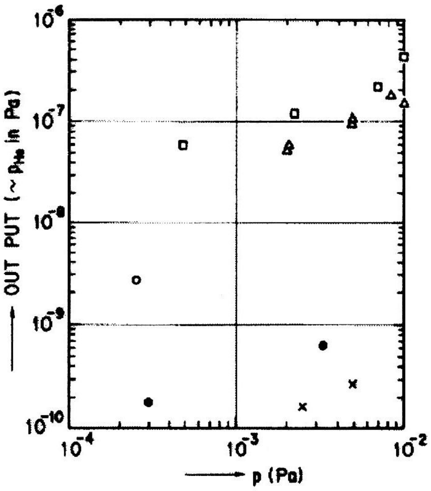

Fig. 6. Sensitivities of helium sensor for main gas species other than helium as a function of pressure (□ ,Δ:H_2, •,○:H_2O, ×:N_2). In cases of Δ, ○ and ×, gas was supplied from the backing line of TMP.

TABLE 4.
Relative sensitivities of helium sensor against other gases.

Gas	Relative sensitivity
H_2	5×10^{-5}
H_2O	5×10^{-7}
N_2	5×10^{-9}

Now, we can estimate pressures at some points in each system and the minimum detectable leak for both systems. The minimum detectable leak means the leak rate in the test chamber when the S/N ratio of the sensor output equals 1. Noise means all kinds of output from sensor amplifier. It includes output caused by gases other than helium and electronic fluctuation of the amplifier. Electronic noise delta Δp_{eq}, of the amplifier is reduced to an equivalent helium pressure. For the estimation of these noise levels, we made a measurement of sensor response for the gases other than helium as well as the zero level fluctuation of output of a commercial counter-flow LD. Figure 6 shows a result of the measurement, and relative sensitivities S_{rel} for hydrogen, water vapour and nitrogen are summarized in Table 4. Then, S/N ratio is given as

$$S/N = p_2(\mathrm{He})/[S_{rel}(\mathrm{H_2})p_2(\mathrm{H_2})+S_{rel}(\mathrm{H_2O})p_2(\mathrm{H_2O})+S_{rel}(\mathrm{N_2})p_2(\mathrm{N_2})+\Delta p_{eq}] \quad (5)$$

in system A, and

$$S/N = p_4(\mathrm{He})/[S_{rel}(\mathrm{H_2})p_4(\mathrm{H_2})+S_{rel}(\mathrm{H_2O})p_4(\mathrm{H_2O})+S_{rel}(\mathrm{N_2})p_4(\mathrm{N_2})+\Delta p_{eq}] \quad (6)$$

in system B. Because the $p_2(\mathrm{He})$ or $p_4(\mathrm{He})$ are proportional to the leak rate L, the minimum detectable leak L_{min} is

$$L_{min} = \frac{L}{S/N}. \quad (7)$$

The final results are summarized in Table 3. It is clear that the counter-flow LD improves S/N ratio by at least one order of magnitude compared with an ordinary LD and that, at the same time, we should pay much care to decrease hydrogen background. It can also be said that the smaller is the pumping speed of common backing pump, the better is the S/N ratio.

3.2. Time constant of response

Response time is anotner important factor in leak detection. Even if the signal is large, it is difficult to find output signal in case of a very long response time. In the following, we analyse pressure change in the system with an initial condition of:

(1) a leak of helium gas occurs suddenly in the test chamber at $t = 0$, and continues with a constant rate L,

(2) at $t = 0$, the whole system is in a good vacuum condition, and we assume $p_i = 0$ $(i = 1, 2)$ in system A and $p_i = 0$ $(i = 1, 2, 3, 4)$ in system B. At time $t > 0$, pressures p_i will rise and finally reach the equilibrium pressure p_{i0}. The set of p_{i0} values in system A is given by Eq. (2), and the set of p_{i0} values in system B by Eq. (4). In the following, we consider each system in detail.

In the system A, the time dependent equations are

$$V_1 \frac{\mathrm{d}p_1}{\mathrm{d}t} = -Sp_1 - C(p_1 - p_2) + L, \quad (8)$$

$$V_2 \frac{\mathrm{d}p_2}{\mathrm{d}t} = -C(p_2 - p_1) - S_L p_2,$$

with an initial condition of $p_1 = p_2 = 0$ at $t = 0$. We can eliminate the constant L by the following transformations

$$p_i' = p_{i0} - p_i, \quad (9)$$

and the result is the matrix equation

$$\begin{pmatrix} \frac{\mathrm{d}p_1^{'}}{\mathrm{d}t} \\ \\ \frac{\mathrm{d}p_2^{'}}{\mathrm{d}t} \end{pmatrix} = \begin{pmatrix} -(S+C)/V_1 & c/V_1 \\ \\ C/V_2 & -(SL+C)/V_2 \end{pmatrix} \begin{pmatrix} p_1^{'} \\ \\ p_2^{'} \end{pmatrix} \tag{10}$$

with initial conditions

$$p_1^{'}(0) = p_{10}, \quad p_2^{'}(0) = p_{20}.$$

Eq. (10) is a linear relation between $\mathrm{d}p_i^{'}/\mathrm{d}t$ and $p_i^{'}$ and can be converted to a diagonal expression by a linear transformation $[T_{ij}]$ from $p_i^{'}$ to $p_i^{''}$. The matrix elements of the $[T_{ij}]$ transformation are the roots of the secular equation

$$\begin{vmatrix} (S+C)/V_1 + x & -C/V_1 \\ -C/V_2 & (S_L+C)/V_2 + x \end{vmatrix} = 0. \tag{11}$$

Denoting the roots of Eq. (11) by $-\lambda_i$ (then λ_i is always positive), we can determine $p_i^{''}$ by solving a set of the following equations

$$\frac{\mathrm{d}p_i^{''}}{\mathrm{d}t} = -\lambda_i p_i \quad (i = 1, 2). \tag{12}$$

Finally we get

$$p_i^{''} = A_i e^{-\lambda_i t}, \tag{13}$$

where A_i is a constant of integration. The inverse transformation of $[T_{ij}]$ gives $p_j^{'}$ as a linear combination of $p_i^{''}$. Now, we pay attention to p_2 or $p_2^{'}$, because our interest is only in the time response of p_2. It is easy to understand that the initial condition of $p_2^{'}$ (or p_2) is $p_2^{'}(0) = p_{20}$ (or $p_2(0) = 0$) and $[\mathrm{d}p_2^{'}(0)/\mathrm{d}t]_{t=0} = 0$ (or $[\mathrm{d}p_2/\mathrm{d}t]_{t=0} = 0$). Therefore, we can determine $p_i^{'}(t)$ in terms of $p_i^{''}(t)$. As the time response of p_2 (or $p_2^{'}$) is given mainly by the term of the longest time constant, the smallest root of Eq.(11) is most important. Substituting a set of practical values in Table 1 for the quantities of the secular equation, we can write the equation as

$$\begin{vmatrix} \frac{300+5.3}{100} - \lambda & -\frac{5.3}{100} \\ -\frac{5.3}{100} & \frac{100+5.3}{0.5} - \lambda \end{vmatrix} = 0. \tag{14}$$

If λ_1 is the smallest root of Eq. (14), we obtain

$$\lambda_1 = 3.05 = 1/0.328,$$

which is very close to 3.053, an absolute value of the smallest diagonal element of the matrix in Eq. (10). The response time constant τ in system A is about $1/\lambda$, which is

$$\tau = 1/\lambda = 0.328 \ \ \mathrm{s}. \tag{15}$$

In the case of system B, too, the logic is almost the same. The starting point of the analysis is the set of simultaneous differential equations:

$$
\begin{aligned}
\frac{\mathrm{d}p_1}{\mathrm{d}t} &= -\frac{1}{V_1}(S+C)p_1 + \frac{C}{V_1}p_2 + L,\\
\frac{\mathrm{d}p_2}{\mathrm{d}t} &= \frac{1}{V_2}Cp_1 - \frac{1}{V_2}(C+S_A)p_2 + \frac{S_A}{V_2 R_A}p_3,\\
\frac{\mathrm{d}p_3}{\mathrm{d}t} &= \frac{1}{V_3}S_A p_2 - \frac{1}{V_3}\left(S_C + \frac{S_A}{R_A} + \frac{S_B}{R_B}\right)p_3 + \frac{1}{V_3}S_B p_4,\\
\frac{\mathrm{d}p_4}{\mathrm{d}t} &= \frac{S_B}{V_4 R_B}p_3 - \frac{1}{V_4}S_B p_4.
\end{aligned}
\tag{16}
$$

We can eliminate L in Eq. (16) by means of a transformation from p_i to $p_i^{'}$ as

$$
p_i^{'} = p_{i0} - p_i, \tag{17}
$$

where p_{i0} are pressures in the stationary state given by Eq. (3). Therefore, the simultaneous differential equations can be reduced to the matrix equation

$$
\begin{pmatrix} \frac{\mathrm{d}p_1^{'}}{\mathrm{d}t} \\ \frac{\mathrm{d}p_2^{'}}{\mathrm{d}t} \\ \frac{\mathrm{d}p_3^{'}}{\mathrm{d}t} \\ \frac{\mathrm{d}p_4^{'}}{\mathrm{d}t} \end{pmatrix}
=
\begin{pmatrix}
-\frac{S+C}{V_1} & \frac{C}{V_1} & 0 & 0 \\
\frac{C}{V_2} & -\frac{S_A+C}{V_2} & \frac{S_A/R_A}{V_2} & 0 \\
0 & \frac{S_A}{V_3} & -\frac{S_C+S_A/R_A+S_B/R_B}{V_3} & \frac{S_B}{V_3} \\
0 & 0 & \frac{S_B/R_B}{V_4} & -\frac{S_B}{V_4}
\end{pmatrix}
\begin{pmatrix} p_1 \\ p_2 \\ p_3 \\ p_4 \end{pmatrix}. \tag{18}
$$

Then, we can easily obtain a secular equation again from Eq. (18):

$$
\begin{vmatrix}
\frac{S+C}{V_1} - \lambda & -\frac{C}{V_1} & 0 & 0 \\
-\frac{C}{V_2} & \frac{S_A+C}{V_2} - \lambda & -\frac{S_A/R_A}{V_2} & 0 \\
0 & -\frac{S_A}{V_3} & \frac{S_C+S_A/R_A+S_B/R_B}{V_3} - \lambda & -\frac{S_B/R_B}{V_3} \\
0 & 0 & -\frac{S_B}{V_4} & \frac{S_B}{V_4} - \lambda
\end{vmatrix} = 0. \tag{19}
$$

The roots of Eq. (19), λ_i, give a full information about the time response of p_4. Note that λ_i are positive. A routine computation gives p_4 as a linear combination of four independent solutions of $B_i \exp(-\lambda_i t)$:

$$
p_4(t) = p_{40} - \sum B_i \exp(-\lambda_i t)
$$

with the initial conditions

$$
[p_4]_{t=0} = 0, \quad \left[\frac{\mathrm{d}p_4^{'}}{\mathrm{d}t}\right]_{t=0} = 0, \quad \left[\frac{\mathrm{d}^2 p_4^{'}}{\mathrm{d}t^2}\right]_{t=0} = 0, \left[\frac{\mathrm{d}^3 p_4^{'}}{\mathrm{d}t^3}\right]_{t=0} = 0. \tag{20}
$$

In this case, too, the smallest value of λ, λ_1 plays the main role in p_4.

Substituting numerical values of Table 2 for the quantities in the secular equation of Eq. (19), we get a numerical equation for λ:

$$\begin{vmatrix} \frac{300+5.3}{100} - \lambda & -\frac{5.3}{100} & 0 & 0 \\ -\frac{5.3}{0.2} & \frac{100+5.3}{0.2} - \lambda & -\frac{100/5500}{0.2} & 0 \\ 0 & -\frac{100}{0.2} & \frac{0.01+100/5500+100/74}{0.2} - \lambda & -\frac{100}{0.2} \\ 0 & 0 & -\frac{100/74}{0.3} & \frac{100}{0.3} - \lambda \end{vmatrix} = 0. \tag{21}$$

According to a numerical calculation, the smallest value of λ is

$$\lambda_1 = 0.121. \tag{22}$$

Here, we introduce a new quantity, the detectability D of a leak detection system:

$$D^{-1} = L_{min}\tau. \tag{23}$$

If a time dependent signal $x(t)$ is approximated in the form of

$$x(t) = A[1 - \exp(-t/\tau)], \tag{24}$$

the initial slope of $x(t)$ is A/τ. Assuming that $x(t)$ is an output signal from the sensor, the signal height A is proportional to the S/N ratio, hence to $(L_{min})^{-1}$. Therefore, the detectability D defined above may be approximated as follows,

$$D = \frac{1}{L_{min}\tau} \sim \frac{A}{\tau}, \tag{25}$$

which is the initial slope of signal $x(t)$. In the leak job, we do not watch the deflection of the meter but its change. This is why we introduced D as a measure of detectability of a leak detection system. It is clear that the value of D of the system B compares well with other systems (Table 3).

4. Summary

We studied two types of leak detection systems among a variety of such systems, and made a detailed analysis of their sensitivity and response time. One is a typical leak detection system with a standard LD, and the other is a system with a newly proposed counter-flow LD. The new type counter-flow LD has TMPs pumped by one small forepump. In the analysis, we introduced two quantities, the minimum detectable leak rate L_{min} and response time constant τ, and evaluated leak detection performance of the two systems. Minimum detectable leak is defined with regard to the signal to noise ratio S/N given in Eq. (7). The evaluated results for the minimum detectable leak L_{min} and the response time constant τ are given in Table 3. We introduced a new quantity, the detectability D of a leak hunting system:

$$D = (\text{minimum detectable leak}) \times (\text{time constant of response}).$$

The quantity D can be defined for a system with a test chamber to be tested, but not for a LD itself. The values of detectability D are also given in Table 3. The value of D shows a good correspondence with the leak–hunting performance of the system.

Acknowledgement

The author would like to express his sincere thanks to Prof. M. Kobayashi of the National Laboratory for High Energy Physics (KEK) for the fruitful discussions with the author. He also extends his thanks to Mr. K. Kakihara of KEK for his help in the experiments.

References

1) W. Becker, Vak. Tech. **17** (1968) 203;

2) G. Reich, J. Vac. Sci. Tech. **A5** (1987) 2641;

3) G. Horikoshi, Y. Saito and K. Kakihara, Vacuum **41** (1990) 2132;

4) O. Taniguchi, H. Suzuki and T. Sawada, Transactions of the Japan Society of Mechanical Engineers **36** (1970) 781.

GRANICA OSJETLJIVOSTI PROTUSTRUJNOG DETEKTORA PROPUSTLJIVOSTI

Izlaže se opći pregled sistema za detekciju propustljivosti vakuumskih uređaja s posebnom pažnjom na turbomolekulsku pumpu s dva ulaza i na nov protustrujni detektor propustljivosti. Radi određivanja učinkovitosti rada tih sustava, raspravlja se minimalno propuštanje koje se može opaziti i vremenska konstanta odziva sustava. Pomoću tih značajki određuju se učinkovitosti raznih uređaja.